

# Dynamical density-density correlations in the one-dimensional Bose gas

Jean-Sébastien Caux and Pasquale Calabrese

*Institute for Theoretical Physics, University of Amsterdam, 1018 XE Amsterdam, The Netherlands.*

(Dated: May 25, 2019)

The zero-temperature dynamical structure factor of the one-dimensional Bose gas with delta-function interaction (Lieb-Liniger model) is computed using a hybrid theoretical/numerical method based on the exact Bethe Ansatz solution, which allows to interpolate continuously between the weakly-coupled Thomas-Fermi and strongly-coupled Tonks-Girardeau regimes. The results should be experimentally accessible with Bragg spectroscopy.

The physics of low dimensional atomic systems presents very special features as compared to the three-dimensional case. As the temperature is lowered, a uniform gas of bosons in three dimensions will undergo a transition to a Bose-Einstein condensate (BEC)<sup>1</sup>; in the one-dimensional case low-energy fluctuations prevent long-range order. For trapped gases, the situation changes and three regimes become possible in 1D<sup>2</sup>: true condensate, quasicondensate, and a strongly-interacting regime, with BEC limited to extremely small interaction between particles. Trapped 1D gases are now accessible experimentally<sup>3,4,5</sup> in all regimes, the most challenging to obtain being the strongly-interacting case<sup>6,7</sup>, which can survive without fast decay due to a reduced three-body recombination rate<sup>8,9</sup> (a consequence of fermionization).

A natural starting point for the theoretical description of one-dimensional atomic gases in this last regime is provided by bosons with delta-function interaction (the Lieb-Liniger model<sup>10</sup>), whose Hamiltonian is given by

$$H = - \sum_{j=1}^N \frac{\partial}{\partial x_j} + 2c \sum_{\langle i,j \rangle} \delta(x_i - x_j) \quad (1)$$

in which  $c > 0$  is the coupling constant, and the sum is over pairs (we have put  $\hbar = 1 = 2m$  for simplicity). For definiteness, we consider a system of length  $L$  with periodic boundary conditions. In the thermodynamic limit, the physics of the model depends on a single parameter  $\gamma = c/n$  where  $n = N/L$  is the particle density. In 1D, in stark contrast to higher dimensions, low densities lead one to the strong-coupling regime of impenetrable bosons, known as the Tonks-Girardeau<sup>11,12</sup> limit.

Although thermodynamic properties of the Lieb-Liniger model are accessible via the Bethe Ansatz<sup>13</sup>, dynamical objects such as time-dependent correlation functions cannot be obtained with this scheme. For example, the zero-temperature density-density correlation function

$$S(x, t) = \langle \rho(x, t) \rho(0, 0) \rangle \quad (2)$$

(in which  $\rho(x) = \sum_{j=1}^N \delta(x - x_j)$ ) has up to now resisted all efforts towards an exact computation. The present paper presents a reliable and efficient method for computing this, based on mixing integrability and numerics.

Many approximate theoretical schemes have been developed to tackle this issue. In the BEC regime, Bogoli-

ubov theory can be used in conjunction with local density, impulse or eikonal approximations<sup>14</sup>. Specifically in 1D, the asymptotics of correlation functions are described by an effective harmonic fluid approach (Luttinger liquid theory)<sup>15</sup>, which can be used to obtain information on static and dynamical correlation functions at zero and nonzero temperature<sup>16,17</sup>. Inversely to asymptotics, a small distance Taylor expansion was also proposed<sup>18</sup>. Yet another possibility is to exploit an exact fermion mapping, and use the Hartree-Fock and generalized random phase approximation to get dynamical correlators near the Tonks-Girardeau limit in a  $1/\gamma$  expansion<sup>19</sup>. Quantum Monte Carlo has been used to numerically obtain the pair distribution function and static structure factor<sup>20</sup>.

In view of the integrability of (1), one could expect to obtain nonperturbative results for objects such as (2). Much recent progress on the computation of correlation functions for this and other 1D quantum integrable models has in fact been achieved through the Algebraic Bethe Ansatz<sup>21,22,23</sup>. In this paper, we wish to present a novel method for obtaining dynamical correlation functions of model (1), which is based on these developments. We will obtain the zero-temperature dynamical density-density correlation function, or more precisely its Fourier transform (the dynamical structure factor (DSF))

$$S(k, \omega) = \int_0^L dx \int dt e^{-ikx+i\omega t} S(x, t) \quad (3)$$

starting directly from the Bethe Ansatz solution, in a way which is reminiscent of recent work by one of us on dynamical spin-spin correlation functions in Heisenberg magnets<sup>24</sup>. All our results are presented in Figures 1-3. The static structure factor  $S(k) = \int \frac{d\omega}{2\pi} S(k, \omega)$  is also obtained as a subset of our results. The DSF itself is experimentally accessible through Bragg spectroscopy<sup>25</sup>, even in the 1D strongly-correlated regime<sup>26</sup>.

By inserting a summation over intermediate states,  $S(k, \omega)$  is transformed into a sum of matrix elements of the density operator in the basis of Bethe eigenstates  $|\alpha\rangle$ ,

$$S(k, \omega) = \frac{2\pi}{L} \sum_{\alpha} |\langle 0 | \rho_k | \alpha \rangle|^2 \delta(\omega - E_{\alpha} + E_0) \quad (4)$$

where  $\rho_k = \sum_{j=1}^N e^{-ikx_j}$ . All of the elements in each term of this sum are fully determined by the Algebraic

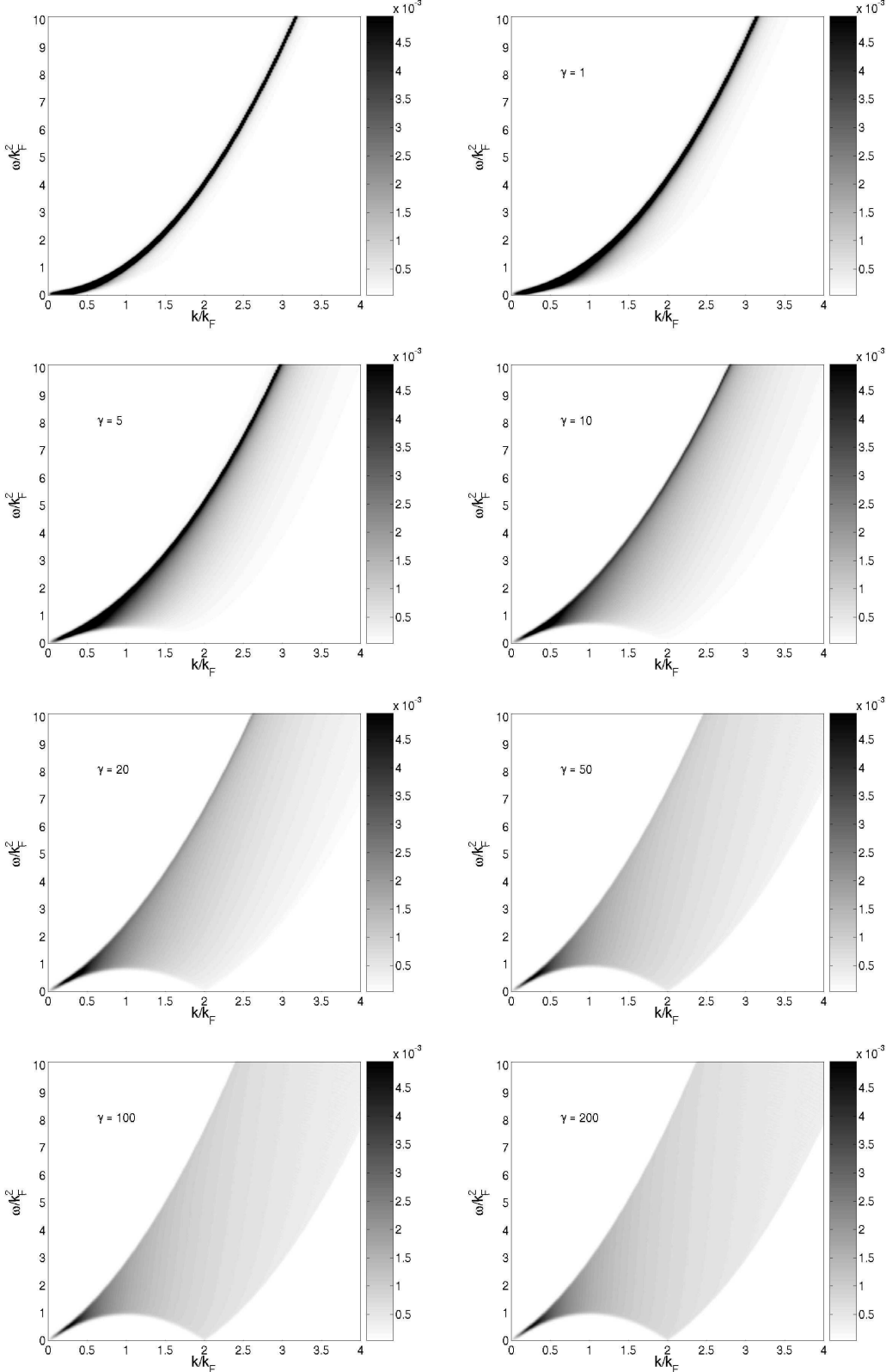


FIG. 1: Density plots of the dynamical structure factor as a function of interaction. The horizontal axis is momentum (running up to  $4k_F$ ), and the vertical axis represents energy transfer. Data obtained from systems of length  $L = 100$  with  $N = 100$  and  $\gamma = 0.25, 1, 5, 10, 20, 50, 100$  and  $200$ .

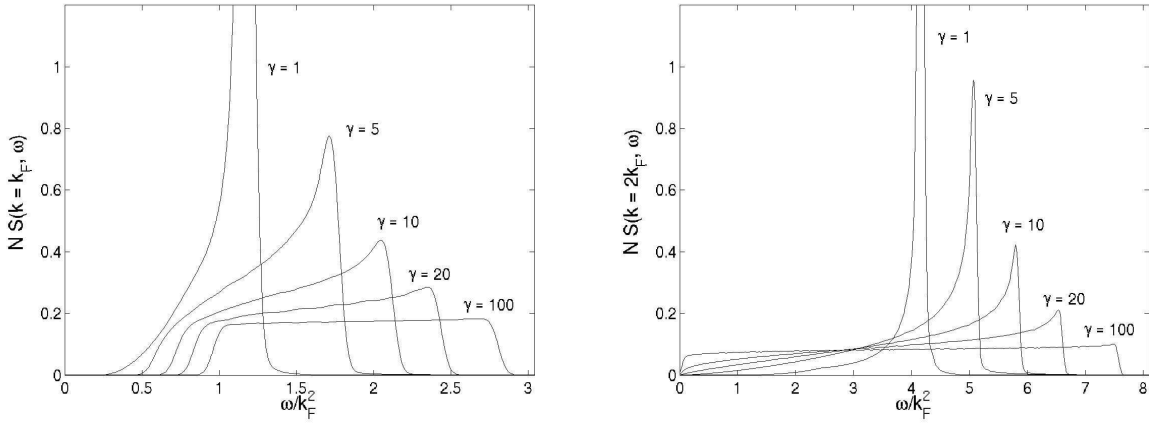


FIG. 2: Fixed momentum plots of the dynamical structure factor for five representative values of the interaction parameter  $\gamma$  obtained using  $L = 100$  and  $N = 100$  (so  $k_F = \pi$ ). The energy  $\delta$ -function in equation (4) is a Gaussian of width  $w = 0.3$ .

Bethe Ansatz, for a finite system with specified boundary conditions as we consider. The Fock space is spanned by the set of Bethe wavefunctions, each fully determined by a set of  $N$  rapidities  $\{\lambda_j\}$ , solution to the Bethe equations

$$\lambda_j + \frac{1}{L} \sum_k 2 \arctan \frac{\lambda_j - \lambda_k}{c} = \frac{2\pi}{L} I_j \quad (5)$$

in which  $I_j$  are half-odd integers (integers) for even (odd)  $N$ . All solutions to these Bethe equations are real. Each set of distinct quantum numbers  $\{I_j\}$ ,  $I_j \neq I_k$  if  $j \neq k$  defines a Bethe eigenstate participating in the sum (4). The energy and momentum of such a state are given by  $E = \sum_j \lambda_j^2$  and  $k = \sum_j \lambda_j = \frac{2\pi}{L} \sum_j I_j$ . The ground-state itself is obtained from the set  $\{I_j^0\}$ , with  $I_j^0 = \frac{N+1}{2} - j$ ,  $j = 1, \dots, N$ . The wavefunction of an eigenstate is given by the Bethe Ansatz, and its norm by the determinant of the Gaudin matrix<sup>27,28</sup>.

Matrix elements of the density operator in the basis of Bethe eigenstates were calculated with the Algebraic Bethe Ansatz in [23]. They are given by the determinant of a matrix whose entries are rational functions of the rapidities of the two eigenstates involved. For the sake of brevity we do not reproduce these expressions here.

What remains to be performed is the actual summation in (4). From this step onwards, everything is done numerically. The Fock space of intermediate states is scanned by navigating through choices of sets of quantum numbers. For each individual intermediate state, the Bethe equations are solved, and the matrix element is computed. To obtain smooth curves in energy, the energy delta function in (4) is broadened to a width equal to a multiple of the typical energy level spacing. The contribution to the dynamical structure factor sum is tallied until good convergence has been achieved. This is quantified by evaluating the  $f$ -sum rule,

$$\int \frac{d\omega}{2\pi} \omega S(k, \omega) = \frac{N}{L} k^2. \quad (6)$$

TABLE I:  $f$ -sum rule saturation percentage achieved at the two representative values of momentum. The method converges fastest in the strongly-interacting regime.

| $\gamma$ | 0.25  | 1     | 5     | 10    | 20    | 50    | 100   | 200   |
|----------|-------|-------|-------|-------|-------|-------|-------|-------|
| $k_F$    | 99.52 | 97.96 | 98.95 | 99.45 | 99.80 | 99.96 | 99.97 | 99.99 |
| $2k_F$   | 99.34 | 96.10 | 96.68 | 98.21 | 99.35 | 99.87 | 99.90 | 99.97 |

Since this is skewed towards high energy, and in view of the ordering of states in the scanning we perform (going from low-energy intermediate states to higher-energy ones), the saturation level of this sum rule represents a lower bound for the saturation of  $S(k, \omega)$  itself.

It is useful to recall here the nature of excitations in the Lieb-Liniger model, which come in two types<sup>10</sup>, Type I (“particles”) and Type II (“holes”)<sup>29</sup>. Type I are Bogoliubov-like quasiparticles that exist for any momentum, and represent states with one quantum number displaced outside the ground-state interval. Their dispersion relation is described in the thermodynamic limit by an integral equation, yielding a curve contained between the asymptotic limits  $\epsilon_I(k) = k^2$  at  $\gamma = 0$  and  $\epsilon_I(k) = k^2 + 2\pi n|k|$  for  $\gamma \rightarrow \infty$ . Type II excitations are holes in the ground-state distribution, and do not appear in Bogoliubov theory. They exist in the interval  $|k| \leq k_F \equiv \pi n$ , and their dispersion relation coincides with the lower threshold of the DSF in the interval  $0 < |k| \leq k_F$ . At  $k = k_F$  they represent zero-energy Umklapp modes. Both dispersion relations approach  $k \rightarrow 0$  with a slope equal to the velocity of sound.

A remarkable feature in this method comes from the fact that it is not necessary to scan through the whole Fock space to get good saturation. Contributions from intermediate states with up to only a handful of particles are sufficient to achieve extremely good accuracy. The saturation of the  $f$ -sum rule (6) achieved for the curves in Figure 2 is summarized in Table 1. Our algorithm is designed to recursively hunt for the most important

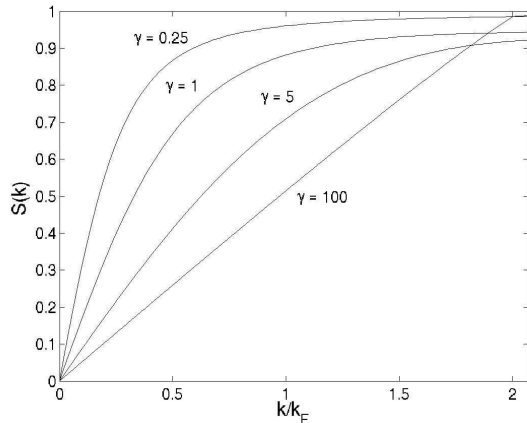


FIG. 3: Static structure factor for four representative values of the interaction parameter  $\gamma$ . All curves saturate to  $S(k \rightarrow \infty) = 1$ .

terms in the multiparticle sum, in decreasing order of contribution to the DSF. Higher accuracy is obtained by using more computational time.

Figure 1 shows density plots for the DSF obtained with our method, for different values of  $\gamma$ . We used unit density  $n = 1$  with  $L = 100$  and  $N = 100$  (this number of particles compares with experimental ones<sup>6,7</sup>). For small  $\gamma$ , the DSF is essentially a single delta peak centered on the Type I dispersion relation,  $S(k, \omega) = \frac{Nk^2}{L\epsilon_I(k)}\delta(\omega - \epsilon_I(k))$ . As  $\gamma$  increases, the DSF progressively flattens until the Tonks-Girardeau limit, where it is constant over a finite frequency interval for

a given momentum. This is illustrated more specifically in Fig. 2. Fig. 3 shows  $S(k)$ , which agrees quantitatively with quantum Monte Carlo results<sup>20</sup> and reproduces the well-known result  $\lim_{\gamma \rightarrow \infty} S(k) = k/2k_F$  for  $k \leq 2k_F$ . Fig. 1 shows that low-energy contributions near  $2k_F$ , which represent superfluidity-breaking Umklapp modes, are important for large  $\gamma$ . For general  $k$ , all the signal lies above the Type II dispersion relation, and multiparticle contributions can in principle give a signal at arbitrarily large energy. In practice, however, the data shows that the smooth onset of the DSF at finite  $\gamma$  is followed by a sharp peak around the Type I dispersion. We believe that in the thermodynamic limit, contributions from intermediate states with higher particle numbers smoothen the upper threshold into a high-frequency tail except in the Tonks-Girardeau limit, where both the lower and upper thresholds remain sharp.

Summarizing, we have computed the dynamical density-density correlation function of the one-dimensional interacting Bose gas (Lieb-Liniger model) for systems with finite numbers of particles, using a Bethe Ansatz-based numerical method. This provides many possible extensions (other correlators, systems with mixed statistics, finite temperatures) on which we will report in future publications.

J.-S. C. acknowledges useful discussions with N. A. Slavnov, M. J. Bhaseen, G. V. Shlyapnikov and J. T. M. Walraven. P. C. acknowledges discussions with M. Polini. This research was supported by the Stichting voor Fundamenteel Onderzoek der Materie (FOM) of the Netherlands.

---

<sup>1</sup> L. Pitaevskii and S. Stringari, “Bose-Einstein Condensation”, Oxford, 2003.

<sup>2</sup> D. S. Petrov, G. V. Shlyapnikov and J. T. M. Walraven, Phys. Rev. Lett. **85**, 3745 (2000).

<sup>3</sup> A. Görlitz *et al.*, Phys. Rev. Lett. **87**, 130402 (2001).

<sup>4</sup> M. Greiner *et al.*, Phys. Rev. Lett. **87**, 160405 (2001).

<sup>5</sup> H. Moritz *et al.*, Phys. Rev. Lett. **91**, 250402 (2003).

<sup>6</sup> B. Paredes *et al.*, Nature **429**, 277 (2004).

<sup>7</sup> T. Kinoshita, T. Wenger and D. S. Weiss, Science **305**, 1125 (2004).

<sup>8</sup> D. M. Gangardt and G. V. Shlyapnikov, Phys. Rev. Lett. **90**, 010401 (2003); K. V. Kheruntsyan *et al.*, Phys. Rev. A **71**, 053615 (2005).

<sup>9</sup> B. Laburthe Tolra *et al.*, Phys. Rev. Lett. **92**, 190401 (2004).

<sup>10</sup> E. H. Lieb and W. Liniger, Phys. Rev. **130**, 1605 (1963); E. H. Lieb, Phys. Rev. **130**, 1616 (1963).

<sup>11</sup> L. Tonks, Phys. Rev. **50**, 955 (1936).

<sup>12</sup> M. Girardeau, J. Math. Phys. (N.Y.) **1**, 516 (1960).

<sup>13</sup> C. N. Yang and C. P. Yang, J. Math. Phys. (N.Y.) **10**, 1115 (1969).

<sup>14</sup> F. Zambelli *et al.*, Phys. Rev. A **61**, 063608 (2000).

<sup>15</sup> F. D. M. Haldane, Phys. Rev. Lett. **47**, 1840 (1981).

<sup>16</sup> A. Berkovich and G. Murthy, Phys. Lett. A **142**, 121 (1989).

<sup>17</sup> D. L. Luxat and A. Griffin, Phys. Rev. A **67**, 043603 (2003).

<sup>18</sup> M. Olshanii and V. Dunjko, Phys. Rev. Lett. **91**, 090401 (2003).

<sup>19</sup> J. Brand and A. Yu. Cherny, Phys. Rev. A **72**, 033619 (2005); A. Yu. Cherny and J. Brand, Phys. Rev. A **73**, 023612 (2006).

<sup>20</sup> G. E. Astrakharchik and S. Giorgini, Phys. Rev. A **68**, 031602(R) (2003).

<sup>21</sup> V. E. Korepin, N. M. Bogoliubov and A. G. Izergin, “Quantum Inverse Scattering Method and Correlation Functions”, Cambridge, 1993, and references therein.

<sup>22</sup> V. E. Korepin, Commun. Math. Phys. **94**, 93 (1984).

<sup>23</sup> N. A. Slavnov, Teor. Mat. Fiz. **79**, 232 (1989); *ibid.*, **82**, 389 (1990).

<sup>24</sup> J.-S. Caux and J. M. Maillet, Phys. Rev. Lett. **95**, 077201 (2005); J.-S. Caux, R. Hagemans and J. M. Maillet, J. Stat. Mech. (2005) P09003.

<sup>25</sup> J. Stenger *et al.*, Phys. Rev. Lett. **82**, 4569 (1999).

<sup>26</sup> T. Stöferle *et al.*, Phys. Rev. Lett. **92**, 130403 (2004).

<sup>27</sup> V. E. Korepin, Commun. Math. Phys. **86**, 391 (1982).

<sup>28</sup> M. Gaudin, “La fonction d’onde de Bethe”, Masson (Paris) (1983).

<sup>29</sup> Although useful for visualizing low-energy excitations, this classification yields double counting (Type II particles are

really a compound of low-momentum Type I particles<sup>10</sup>). The Fock space itself is spanned by using only Type I.